PAPER Special Section on Dynamic Spectrum Access

Time-Frequency Channel Parameterization with Application to Multi-Mode Receivers

Thomas HUNZIKER[†a)], ***Member***, **Ziyang JU**[†], ***and*** **Dirk DAHLHAUS**[†], ***Nonmembers***

SUMMARY There is a trend towards flexible radios which are able to cope with a range of wireless communication standards. For the integrated processing of widely different signals — including single-carrier, multi-carrier, and spread-spectrum signals — monolithic baseband receivers need universal formats for the signal representation and channel description. We consider a reconfigurable receiver architecture building on concepts from time-frequency (TF) signal analysis. The core elements are TF signal representations in form of a Gabor expansion along with a compatible parameterization of time-variant channels. While applicable to arbitrary signal types, the TF channel parameterization offers similar advantages as the frequency domain channel description employed by orthogonal frequency-division multiplexing receivers. The freedom in the choice of the underlying analysis window function and the scalability in time and frequency facilitate the handling of diverse signal types as well as the adaptation to radio channels with different delay and Doppler spreads. Optimized window shapes limit the inherent model error, as demonstrated using the example of direct-sequence spread-spectrum signaling.

key words: *reconfigurable radio, doubly dispersive channel, time-frequency analysis, Gabor expansion, waveform design*

1. Introduction

The emergence of ever new standards for wireless access and networking is fueling the trend towards transceiver devices with multi-mode capabilities. Since the assembling of tailored solutions for single standards into hybrid devices has clear limitations, there is an increasing demand for flexible multi-purpose transceivers which can cope with today's predominant and even potential future air interfaces in an integrated fashion. On the physical layer the challenge is to deal with the various signal formats such as single-carrier, multi-carrier, and spread-spectrum signals. Fundamentally different approaches are followed in traditional radios depending on whether the information-bearing pulses are localized in time, encoded into sub-bands, or spread over time and frequency. Time domain equalizers are typically used for information recovery in single-carrier systems, whereas orthogonal frequency-division multiplexing (OFDM) signals are naturally processed in the frequency domain. The discrete Fourier transform (DFT) yields a signal representation which facilitates straightforward demodulation of broad-band signals. The simple processing in the receivers without a need for complex equalizers, along with the availability of fast Fourier transform (FFT) algorithms, have led to the popularity of OFDM.

A signal representation with similar advantages, yet applicable to both OFDM and non-OFDM signals, would be of great value for reconfigurable monolithic baseband receivers. The block-wise Fourier transform is adequate only for stationary signals — like OFDM signals, which preserve stationarity through cyclic extensions — but lacks desired frequency resolution in cases of transient signals. Better results in this respect are obtained by the short-time Fourier transform (STFT) if based on a smoothly shaped analysis window. The STFT yields a linear time-frequency (TF) representation, the sampled version of which offers efficient representations of the information contents of transient signals [1]. From the discretized TF representation the time domain signal can be expressed by means of an appropriate synthesis window function in a form known as *Gabor expansion* [2], provided the analysis window and the sampling intervals fulfill certain conditions to be discussed below. Computationally efficient implementations of the analysis and synthesis operations associated with the discrete-time Gabor expansion are known from filter bank theory [3]. The so-called polyphase representation leads to implementations which can likewise benefit from FFT algorithms.

In addition to a scalable signal representation, reconfigurable receivers need a suitable format for the description of time-variant radio channels. The usually encountered channels in mobile radio applications are *underspread* channels, which can be regarded as *locally* TF non-selective. This feature lets the signal mapping by the channel be efficiently formulated as a scalar multiplication of each coefficient of the TF signal representation by the channel gain at the respective TF location [4]. This concept for parameterizing linear channels can be seen as a generalization of the "single-tap" channel description known from OFDM towards arbitrary signals without cyclic extensions. In the general case of doubly dispersive channels, such a TF channel model is subject to a certain model error, the magnitude of which can be limited by choosing an adequate window with high TF localization for the signal analysis. A main concern of this paper is to define optimized TF signal representations for channels with known statistical properties, and to demonstrate how these can be taken advantage of in flexible receiver architectures.

1.1 Related Work

Frequency domain equalization (FDE): This widely known

Manuscript received April 15, 2009.
Manuscript revised August 5, 2009.

[†]The authors are with the Communications Laboratory, University of Kassel, Wilhelmshöher Allee 73, Kassel, Germany.
a) E-mail: hunziker@uni-kassel.de

DOI: 10.1587/transcom.E92.B.3717

concept resorts to the frequency domain for recovering signals distorted in time-invariant channels. In [5] the computational complexities of time and frequency domain equalizers are compared, concluding that FDE is simpler when the length of the channel impulse response exceeds the sample time by a factor of 5 or more. Like OFDM receivers, block-wise FDE in general benefits from the simple channel inversion operation and efficient FFT algorithms. Single-carrier modulation with FDE can achieve similar performance as OFDM if a proper cyclic prefix is appended to each block of signals [6]. Processing signals without cyclic prefix results in errors at the block boundaries. These errors have a limited impact at sufficiently large block sizes, making FDE an interesting alternative for code-division multiple access (CDMA) receivers [7], [8]. Alternatively, overlap-save or overlap-add signal processing techniques can be employed. However, all these methods are suitable only for time-invariant channels.

Filter bank-based multi-carrier systems: To get rid of the rigid framework of rectangular windows and cyclic prefixes in OFDM systems, filter banks can be employed for the signal synthesis at the transmitter end as well as the signal analysis at the receiver end [9]–[13]. Interference between adjacent sub-bands or multi-carrier symbols can be avoided, or at least limited, by choosing appropriate transmit pulses. At the receiver end the advantages over conventional OFDM include reduced susceptibility to Doppler spreads, phase noise, and certain forms of cochannel interference [14]. Pulse shapes for minimizing interference are designed in [9], [12], [15], while suitable detection methods for non-orthogonal multi-carrier signaling are discussed in [11], [16].

Software defined radio (SDR): Transceivers with multi-mode capabilities are the proclaimed objective of SDR. Albeit defined as "radio in which some or all of the physical layer functions are software defined" [17], most of the SDR literature (see, e.g., [18] and references therein) focuses on flexible radio front ends, higher layer issues such as radio resource management, and architectural concepts. For the signal demodulation and decoding tasks some form of hardware acceleration seems inevitable in view of the high complexity. Rather than by means of software download, multi-mode capability can be enabled through receivers building on reconfigurable hardware elements, a concept considered in [19] and also advocated in this paper.

1.2 Outline of This Paper

In Sect. 2 the mathematical concepts for the TF representation and processing of signals are introduced. A TF channel parameterization is proposed in Sect. 3, letting the signal distortion in dispersive channels be modeled in a way compatible with the Gabor expansion. A certain model error results in the case of doubly dispersive channels. Expressions of the model error are used in Sect. 4 to derive optimized window functions. In Sect. 5, a generic receiver architecture is presented, the viability of which is discussed for the cases of CDMA and OFDM systems in Sect. 6 including imperfect pilot signal-based channel estimation. Finally, conclusions are drawn in Sect. 7.

1.3 Notation

We use boldfaced characters (e.g., $\mathbf{X}$) for denoting functions which map elements from a discrete domain Λ onto $\mathbb{C}$ and write the function value at $i \in \Lambda$ as $\mathbf{X}_i$. The Hilbert spaces of the square integrable functions $f : \mathbb{R} \to \mathbb{C}$ and the square summable functions $\mathbf{X} : \Lambda \to \mathbb{C}$ are denoted as $L^2(\mathbb{R})$ and $L^2(\Lambda)$, respectively, with their respective inner products $\langle f, g\rangle$ and $\langle \mathbf{X}, \mathbf{Y}\rangle$ defined as $\int_{\mathbb{R}} fg^*$ and $\sum_{i\in\Lambda} \mathbf{X}_i\mathbf{Y}_i^*$, where the asterisk in the superscript denotes complex conjugation, and the L^2-norms $\|f\| \triangleq \sqrt{\langle f, f\rangle}$ and $\|\mathbf{X}\| \triangleq \sqrt{\langle \mathbf{X}, \mathbf{X}\rangle}$. Furthermore, we let $\odot$ denote the one-by-one multiplication of two compatible functions $\mathbf{X}, \mathbf{Y}$, i.e., if $\mathbf{Z} = \mathbf{X} \odot \mathbf{Y}$ then $\mathbf{Z}_i = \mathbf{X}_i\mathbf{Y}_i \ \forall i \in \Lambda$. Also, $E[\cdot]$ denotes expectation and $j \triangleq \sqrt{-1}$.

2. Time-Frequency Signal Representation

Given a window function $g \in L^2(\mathbb{R})$ and two positive constants T and F, the set

$$\{g_{k,\ell}(t) \ : \ (k,\ell) \in \Lambda\} \text{ with}$$
$$g_{k,\ell}(t) \triangleq g(t - kT)\exp(j2\pi(t - kT)\ell F) \tag{1}$$

and $\Lambda \triangleq \mathbb{Z} \times \mathbb{Z}$ is referred to as a *Gabor system*. The elements of the Gabor system can be seen as relating to the grid points $\{(kT, \ell F) : (k,\ell) \in \Lambda\}$ of a lattice overlaying the TF plane. The intervals T and F at which the elements are spaced in time and frequency, respectively, are called the *lattice constants*. For an arbitrary $x \in L^2(\mathbb{R})$ the inner products of $x(t)$ with every element of the Gabor system form a linear TF representation. This transform is in the following represented by the analysis operator

$$\mathcal{G} : x(t) \mapsto \mathbf{X}, \quad \mathbf{X}_{(k,\ell)} \triangleq \langle x, g_{k,\ell}\rangle, \quad (k,\ell) \in \Lambda. \tag{2}$$

Reconstruction of $x(t)$ from its TF representation $\mathcal{G}x$ is generally possible if (1) constitutes a *Gabor frame*. Formally, the triplet $(g(t), T, F)$ with associated analysis operator $\mathcal{G}$ defines a Gabor frame (also sometimes called *Weyl-Heisenberg frame*) if there exist two constants $A, B > 0$ such that

$$A\|x\|^2 \le \|\mathcal{G}x\|^2 \le B\|x\|^2 \quad \forall x \in L^2(\mathbb{R}). \tag{3}$$

If (3) holds with $A = B = 1$, then (1) represents a normalized *tight* Gabor frame. These special Gabor frames are of prime interest since they obey a generalized Parseval's identity

$$\|x\|^2 = \|\mathcal{G}x\|^2 \quad \forall x \in L^2(\mathbb{R}). \tag{4}$$

Furthermore, the inner product $\langle x, y\rangle$ of any two $x, y \in L^2(\mathbb{R})$ can be computed on the basis of the respective TF representations $\mathcal{G}x$ and $\mathcal{G}y$, that is,

$$\langle x, y\rangle = \langle \mathcal{G}x, \mathcal{G}y\rangle \quad \forall x, y \in L^2(\mathbb{R}). \tag{5}$$

A necessary condition for $(g(t), T, F)$ to define a Gabor frame is that $TF \leq 1$, and for normalized tight frames additionally $\|g\|^2 = TF$. For a discussion of these conditions and more insight into Gabor analysis the reader is referred to the rich literature, for instance [2], [20].

In the rest of the paper we assume that $(g(t), T, F)$ constitutes a normalized tight frame. Adopting the mathematical concept of tight frames for the TF representation of signals, the properties (4) and (5) are of central importance as they let baseband receivers perform operations for the signal demodulation, such as signal energy computations and correlations against reference waveforms, directly in the TF domain.

3. Time-Frequency Channel Parameterization

The mapping $\mathcal{H} : L^2(\mathbb{R}) \to L^2(\mathbb{R})$ of an input signal $x(t)$ onto the signal $y(t) \triangleq (\mathcal{H}x)(t)$ at the output of a linear, time-variant channel can be expressed as

$$y(t) = \int_{-\infty}^{\infty} c_{\mathcal{H}}(t, s)x(s)ds. \tag{6}$$

The kernel $c_{\mathcal{H}}(t, s)$ is related to the time-variant impulse response $h_{\mathcal{H}}(\tau; t)$ through $h_{\mathcal{H}}(\tau; t) = c_{\mathcal{H}}(t, t-\tau)$. The TF selectivity of the channel is reflected by the time-variant transfer function $C_{\mathcal{H}}(t, f)$, which is obtained from the kernel through

$$C_{\mathcal{H}}(t, f) = \int_{-\infty}^{\infty} c_{\mathcal{H}}(t, t-\tau)\exp(-j2\pi f\tau)d\tau, \quad (t, f) \in \mathbb{R}\times\mathbb{R}. \tag{7}$$

For stochastic channels, $C_{\mathcal{H}}(t, f)$ represents a two-dimensional random process. Zero-mean and wide-sense stationarity are often assumed for $C_{\mathcal{H}}(t, f)$ with respect to both t and f. Expressing the two-dimensional autocorrelation as

$$E\left[C_{\mathcal{H}}(t, f)C^*_{\mathcal{H}}(t', f')\right] = R_{\mathcal{H}}(t - t', f - f') = R_{\mathcal{H}}(t_\Delta, f_\Delta) \tag{8}$$

leads to a wide-sense stationary uncorrelated scattering (WSSUS) model [21] of $h_{\mathcal{H}}(\tau; t)$. The slope of $R_{\mathcal{H}}(t_\Delta, f_\Delta)$ in the time dimension relates to the coherence time, while the slope in the frequency dimension relates to the coherence frequency of the channel. The dispersiveness of the channel is further reflected by the scattering function, which is obtained from $R_{\mathcal{H}}(t_\Delta, f_\Delta)$ through a two-dimensional Fourier transform.

In a digital signal processor a doubly dispersive channel realization can be represented by the sampled version $\mathbf{H}$ of $C_{\mathcal{H}}(t, f)$, defined by

$$\mathbf{H}_{(k,\ell)} \triangleq C_{\mathcal{H}}(kT, \ell F), \quad (k, \ell) \in \Lambda. \tag{9}$$

For compatibility with the TF signal representations introduced in the previous section, the sampling intervals are chosen in line with the abovementioned lattice constants T and F. The time-variant transfer function exhibits the complex-valued channel gain over time and frequency. Hence, given the TF representation $\mathbf{X} \triangleq \mathcal{G}x$ of a signal $x(t)$ at the channel input, it is straightforward to represent the signal $y(t)$ at the channel output as

$$\widehat{\mathbf{Y}} = \mathbf{H} \odot \mathbf{X}. \tag{10}$$

We note the similarity of (10) with expressions for the DFT output in OFDM receivers. The formulation of the signal mapping by the channel as an element-wise multiplication by $\mathbf{H}$ facilitates scalable and efficient receiver processing known from OFDM. However, as a result of the sampling of $C_{\mathcal{H}}(t, f)$ the model (10) is usually only approximative, and $\widehat{\mathbf{Y}}$ an approximation of $\mathbf{Y} \triangleq \mathcal{G}y$. The accuracy of (10) depends on the channel characteristics and the operator $\mathcal{G}$. We may expect the model error to be limited if every elementary function $g_{k,\ell}(t)$ is concentrated around $(kT, \ell F)$ in the TF plane such that $C_{\mathcal{H}}(t, f)$ is essentially constant within the sphere of $g_{k,\ell}(t)$. Window functions fulfilling this can be designed for the typical underspread channel encountered in mobile radio scenarios, as shown in Sect. 4. While a requirement is that $TF \leq 1$, tight frames with desirable properties in regard to TF concentration are only feasible if the product TF is strictly smaller than 1 [2]. Regarding time and frequency dispersion by an underspread channel as symmetrical effects, the sampling intervals T and F are best chosen such that they are proportional to the coherence time and frequency, respectively. Besides of environmental factors, however, in flexible receiver applications the choice of T and F may be constrained by signal properties such as symbol length or subcarrier spacing.

4. Optimized Gabor Systems

In this section we investigate the model error associated with the above proposed TF channel parameterization. Mean-squared error expressions are derived in Sect. 4.1 for channels with known statistics. These serve as objective functions in the design of optimized Gabor systems, using suitable numerical optimization methods as discussed in Sect. 4.2.

4.1 Model Error Expressions

For the assessment of the model error, consider the setup in Fig. 1. Given a random input signal $x(t)$, the TF representation $\mathbf{Y}$ of the actual signal $y(t)$ at the output of a random channel appears at the right hand side end of the upper chain, whereas in the lower chain the channel output is re-

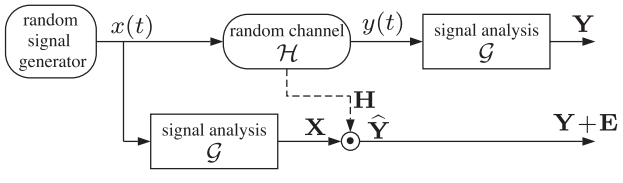

Fig. 1 Setup for window optimization.

produced by a signal analysis (2) followed by a coefficient-wise multiplication as per (10)†. To remain general in regard to signal and channel properties, we consider the error signal $\mathbf{E} \triangleq \widehat{\mathbf{Y}} - \mathbf{Y}$ under the assumptions of

- a white random signal $x(t)$ with unit power spectral density at the channel input,
- a random channel $\mathcal{H}$ complying with the WSSUS model, with unit average channel gain, i.e., $R_{\mathcal{H}}(0,0) = 1$.

The mean-squared coefficient error (MSCE) $\varepsilon_{\mathrm{MSCE}}{}^{(k,\ell)}(g) \triangleq E[|\mathbf{E}_{(k,\ell)}|^2]$ is given as

$$\varepsilon_{\mathrm{MSCE}}{}^{(k,\ell)}(g) = E\left[\left|\mathbf{H}_{(k,\ell)}\langle x, g_{k,\ell}\rangle - \langle \mathcal{H}x, g_{k,\ell}\rangle\right|^2\right]. \quad (11)$$

In the following we omit the TF index (k,ℓ) since the MSCE is independent of $(k,\ell) \in \Lambda$ as a result of the wide-sense stationarity of $C_{\mathcal{H}}(t,f)$. Making use of the above assumptions, the error can be expressed as

$$\varepsilon_{\mathrm{MSCE}}(g) = 2\left(TF - \Re\left(\int_{-\infty}^{\infty}\int_{-\infty}^{\infty} R_{\mathcal{H}}(t,f) Z_g^*(t,f) df dt\right)\right) \quad (12)$$

as shown in the appendix. The so-called *Rihaczek distribution* $Z_g(t,f)$ of $g(t)$ is defined as

$$Z_g(t,f) = g(t)\int_{-\infty}^{\infty} g^*(t-\tau) e^{-j2\pi f\tau} d\tau. \quad (13)$$

Note that the argument of the real part operator $\Re(\cdot)$ in (12) represents a two-dimensional inner product, where $R_{\mathcal{H}}(t,f)$ reflects the channel statistics and $Z_g(t,f)$ depends on the window $g(t)$. The function $Z_g(t,f)$ can be seen as the complex energy density distribution of $g(t)$ over time and frequency [23], satisfying $\int_{-\infty}^{\infty}\int_{-\infty}^{\infty} Z_g(t,f) df dt = \|g\|^2$. For TF non-selective channels, $R_{\mathcal{H}}(t,f) = 1$ and thus $\varepsilon_{\mathrm{MSCE}}(g) = 0$.

The usually encountered channels in mobile radio applications are TF selective. The expression (12) can be rewritten as

$$\varepsilon_{\mathrm{MSCE}}(g) = 2\left(TF - \int_{-\infty}^{\infty}\int_{-\infty}^{\infty} g^*(t) P_{\mathcal{H}}(t,t') g(t') dt dt'\right) \quad (14)$$

with $P_{\mathcal{H}}(t,t')$ a Hermitian kernel function defined as

$$P_{\mathcal{H}}(t,t') = \frac{1}{2}\int_{-\infty}^{\infty}\left(R_{\mathcal{H}}(t,f) + R_{\mathcal{H}}^*(t',f)\right) e^{j2\pi f(t-t')} df. \quad (15)$$

Recalling that $\|g\|^2 = TF$, the MSCE can obviously be lower bounded as $\varepsilon_{\mathrm{MSCE}}(g) \geq 2TF(1 - \lambda_{\max}^{(\mathcal{H})})$, where $\lambda_{\max}^{(\mathcal{H})}$ denotes the largest eigenvalue of the Hermitian kernel function (15).

We now consider the relative mean-squared model error (RMSME) $\varepsilon_{\mathrm{RMSME}}(g) \triangleq E[\|\mathbf{E}\|^2]/E[\|\mathbf{Y}\|^2]$. To keep $\|\mathbf{E}\|^2$ and $\|\mathbf{Y}\|^2$ finite, let us first redefine Λ as the finite index set $\{0,\ldots,K-1\} \times \{0,\ldots,L-1\}$ with K, L large integer constants. Now, $E[\|\mathbf{E}\|^2] = KL\varepsilon_{\mathrm{MSCE}}(g)$, whereas $E[\|\mathbf{Y}\|^2] = KLTF$ as follows from the unit channel gain and $\|g\|^2 = TF$. Hence,

$$\varepsilon_{\mathrm{RMSME}}(g) = \frac{\varepsilon_{\mathrm{MSCE}}(g)}{TF}. \quad (16)$$

The RMSME (16) naturally characterizes the model error even for Λ an infinite index set. Of central interest is the order of magnitude to which the RMSME can be confined by optimal design of $g(t)$ given the lattice constants and channel statistics. As follows from the above derived lower bound on $\varepsilon_{\mathrm{MSCE}}(g)$,

$$\varepsilon_{\mathrm{RMSME}}(g) \geq 2\left(1 - \lambda_{\max}^{(\mathcal{H})}\right). \quad (17)$$

Note that $\lambda_{\max}^{(\mathcal{H})}$ depends only on the channel statistics. As easily seen, we have $\lambda_{\max}^{(\mathcal{H})} \in (0,1)$ for doubly dispersive channels, hence, a certain model error remains even with optimized window functions and arbitrarily small sampling intervals T and F.

4.2 Numerical Window Optimization

Discretization of the window function $g(t)$ and $P_{\mathcal{H}}(t,t')$ leads to a matrix formulation of the MSCE in the form $\varepsilon_{\mathrm{MSCE}}(\mathbf{g}) = \mathbf{g}^{\mathrm{H}}\mathbf{B}\mathbf{g}$, where the vector $\mathbf{g}$ defines the synthesis window of a discrete-time Gabor expansion [24] and $(\cdot)^{\mathrm{H}}$ denotes Hermitian transposition. As follows from (14) and the fact that the error cannot become negative, the matrix $\mathbf{B}$ is Hermitian positive semidefinite, which we write as $\mathbf{B} \geq 0$. Alternatively the objective function can be expressed as $\varepsilon_{\mathrm{MSCE}}(\mathbf{g}) = \mathrm{tr}(\mathbf{B}\mathbf{G})$ with $\mathbf{G} \triangleq \mathbf{g}\mathbf{g}^{\mathrm{H}}$ and $\mathrm{tr}(\cdot)$ denoting the trace. This form is particularly accessible for *semidefinite programming* (SDP), a special form of convex optimization. By SDP, optimization problems of the form

$$\mathbf{G}_{\mathrm{opt}} = \arg\min_{\mathbf{G}} \mathrm{tr}(\mathbf{B}\mathbf{G}) \quad \text{subject to} \quad \begin{cases} \mathbf{G} \geq 0, \\ \mathrm{tr}(\mathbf{A}^{(i)}\mathbf{G}) = b_i \;\; i = 1,\ldots,N \end{cases} \quad (18)$$

can be solved. By means of the N constraints imposed by the matrices $\mathbf{A}^{(1)},\ldots,\mathbf{A}^{(N)}$ and scalars $b_1,\ldots,b_N$ the window $\mathbf{g}$ can be enforced to define a tight Gabor frame as shown in [25], [26].

If the rank of $\mathbf{G}_{\mathrm{opt}}$ turns out to be 1, a window $\mathbf{g}_{\mathrm{opt}}$ defining a tight frame resulting in minimal MSCE is readily obtainable from $\mathbf{G}_{\mathrm{opt}} = \mathbf{g}_{\mathrm{opt}}\mathbf{g}_{\mathrm{opt}}^{\mathrm{H}}$. Otherwise, rank reduction methods need to be applied on $\mathbf{G}_{\mathrm{opt}}$ which usually result in a suboptimal solution of the optimization problem [25].

4.3 Numerical Results

The matrix $\mathbf{B}$ resulting from discretization of (15) reflects the second-order channel statistics. Assuming the WSSUS model along with a separable scattering function, we have

†Concatenations of these two operations and an additional synthesis operation for the purpose of approximating a linear operator appear in the literature under the name *Gabor multiplier*. Given a linear operator, methods are presented in [22] for computing Gabor systems which minimize the approximation error. However, these methods are not applicable in our context since we assume that the linear operator (i.e., the channel $\mathcal{H}$) is random rather than deterministic.

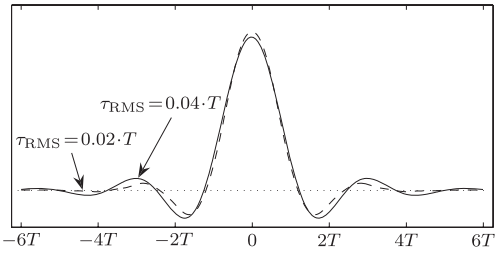

Fig. 2 Window functions for TF signal analysis optimized for doubly dispersive channels with given second-order statistics.

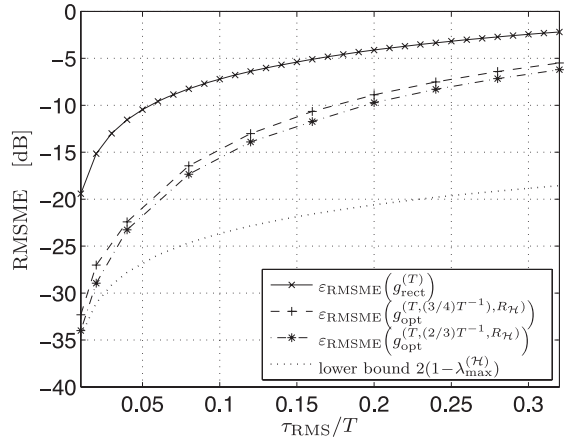

Fig. 3 Model errors $\varepsilon_{\mathrm{RMSME}}(g_{\mathrm{opt}}^{(T,F,R_{\mathcal{H}})})$ and $\varepsilon_{\mathrm{RMSME}}(g_{\mathrm{rect}}^{(T)})$ by optimized windows and rectangularly shaped window, respectively, and corresponding lower bound (17) versus relative RMS delay spread.

$R_{\mathcal{H}}(t_\Delta, f_\Delta) = \phi_{\mathrm{t}}(t_\Delta)\phi_{\mathrm{f}}(f_\Delta)$ with $\phi_{\mathrm{t}}(t_\Delta)$ and $\phi_{\mathrm{f}}(f_\Delta)$ representing the time and frequency correlation functions. These are given as $\phi_{\mathrm{t}}(t_\Delta) = \int_{-\infty}^{\infty} S_{\mathrm{Doppler}}(\nu)\exp(j2\pi t_\Delta \nu)d\nu$ and $\phi_{\mathrm{f}}(f_\Delta) = \int_{-\infty}^{\infty} S_{\mathrm{delay}}(\tau)\exp(-j2\pi f_\Delta \tau)d\tau$ with the real non-negative functions $S_{\mathrm{delay}}(\tau)$ and $S_{\mathrm{Doppler}}(\nu)$ representing the delay and Doppler power spectra, respectively. Figure 2 shows two examples of optimized window functions. The waveforms were obtained by SDP under the assumptions of $TF = \frac{3}{4}$ and exponentially decaying delay and two-sided exponentially decaying Doppler power spectra given by $S_{\mathrm{delay}}(\tau) = u(\tau)\exp(-\tau/\tau_{\mathrm{RMS}})$ with $u(\tau)$ denoting the unit step function and $S_{\mathrm{Doppler}}(\nu) = \exp(-\sqrt{2}|\nu|/\nu_{\mathrm{RMS}})$, respectively. Root mean-squared (RMS) delay spreads τ_{RMS} of 0.02 and 0.04 relative to T were assumed, and an RMS Doppler spread of 0.005 relative to $1/T$ (i.e., $\nu_{\mathrm{RMS}} = 0.005/T$) for the sake of compatibility with the case study in Sect. 6.1.

The achievable RMSMEs (16) by windows $g_{\mathrm{opt}}^{(T,F,R_{\mathcal{H}})}(t)$ optimized for given $(T, F, R_{\mathcal{H}}(\cdot,\cdot))$ are shown in Fig. 3 for the above described power spectra, $TF = \frac{3}{4}$ and $TF = \frac{2}{3}$, and an RMS Doppler spread ν_{RMS} of $0.005/T$. The numerically computed RMSMEs are shown in the figure for RMS delay spreads between $0.01 \cdot T$ and $0.32 \cdot T$. Additionally, the figure shows the corresponding lower bounding values $2(1-\lambda_{\max}^{(\mathcal{H})})$, and also the RMSMEs resulting from choosing a rectangularly shaped window $g_{\mathrm{rect}}^{(T)}(t)$ and $TF = 1$, where $g_{\mathrm{rect}}^{(T)}(t) \triangleq T^{-\frac{1}{2}}$ for $t \in [-\frac{T}{2}, \frac{T}{2})$ and 0 for $t \notin [-\frac{T}{2}, \frac{T}{2})$. The latter choice lets (1) constitute an orthonormal basis, and in discrete-time the associated analysis and synthesis operations are implemented as block-wise DFTs and inverse DFTs, respectively.

Obviously, even a relatively small signal dispersion by the channel in the time dimension has a significant impact on the RMSME in the case of a rectangularly shaped window function. Optimized window shapes result in much better performance. This indicates that the error resulting from the block-wise processing of signals without proper cyclic extensions can be limited by resorting to appropriate TF signal representations as compared to conventional frequency domain processing. However, the constraint on the window function to define a tight Gabor frame results in a considerable distance to the lower bound in cases of larger delay spreads.

5. Generic Receiver Architectures

Unlike channel parameterization in conventional OFDM, rake CDMA, and other mode-specific receivers, the above considered TF channel model does not rely on a particular signal format, making it suitable for application in multi-mode receivers. In the following, a flexible baseband receiver architecture is discussed which incorporates the TF channel model. The inner receiver performs matched filtering and pulse cross-correlation computations in the TF domain, facilitating demodulation and decoding by standard methods in the outer receiver.

The burst structures defined in the various standards for cellular systems and wireless local and personal area networks differ substantially. However, commonly the bursts incorporate preamble and pilot signals for the synchronization and channel parameter estimation, and information-bearing signals which are usually subject to a linear modulation scheme. The baseband transmit signals generally follow the form

$$x(t) = \sum_{m=1}^{M} s_m z_m(t) + p(t) \tag{19}$$

with $s_1, \ldots, s_M$ denoting M information signals which modulate the elementary waveforms $z_1(t), \ldots, z_M(t)$, and $p(t)$ a preamble/pilot signal. An elementary waveform can be a complex exponential as in the case of OFDM, or have the form of a pseudo-noise sequence as in the case of direct-sequence spread-spectrum (DSSS) signaling. The pilot/preamble signal may be confined to isolated time intervals, or exhibit constant power as in the case of a CDMA system with a dedicated pilot channel. The baseband signal at the receiver reads

$$y(t) = (\mathcal{H}x)(t) + v(t), \tag{20}$$

where $v(t)$ represents the additive front end noise. Note that the TF representation of $y(t)$ can be written as

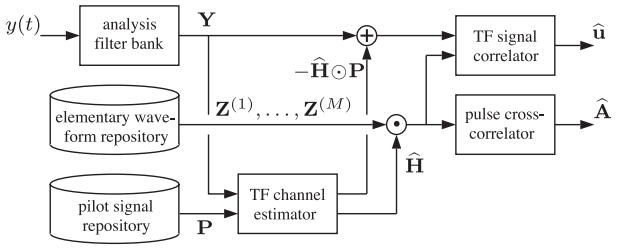

Fig. 4 Generic inner baseband receiver structure.

$$\mathbf{Y} = \mathbf{H} \odot \left(\sum_{m=1}^{M} s_m \mathbf{Z}^{(m)} + \mathbf{P} \right) + \mathbf{W} \tag{21}$$

with $\mathbf{Z}^{(m)} \triangleq \mathcal{G} z_m$ and $\mathbf{P} \triangleq \mathcal{G} p$ representing the mth information signal and the pilot signal, respectively, and $\mathbf{W}$ the noise $v(t)$ together with the inherent error from the channel parameterization.

Matched filtering of the information-bearing part $y(t) - (\mathcal{H}p)(t)$ of the received signal against the M distorted waveforms yields

$$u_m = \langle y - \mathcal{H}p, \mathcal{H}z_m \rangle, \quad m = 1, \ldots, M. \tag{22}$$

The coefficients $u_1, \ldots, u_M$ represent a sufficient statistic for the decoding problem under the assumption of $v(t)$ representing an additive white Gaussian noise (AWGN) process. As easily seen, the vector $\mathbf{u}$ comprising $u_1, \ldots, u_M$ can be expressed as

$$\mathbf{u} = \mathbf{A}\mathbf{s} + \mathbf{v}, \tag{23}$$

where the vector $\mathbf{s}$ comprising the signals $s_1, \ldots, s_M$ represents the transmitted codeword, $\mathbf{A}$ denotes the pulse cross-correlation matrix, and the noise vector $\mathbf{v}$ contains $\langle v, \mathcal{H}z_1 \rangle, \ldots, \langle v, \mathcal{H}z_M \rangle$. The nth element of the mth row of the $M \times M$-matrix $\mathbf{A}$ is given as

$$a_{m,n} = \langle \mathcal{H}z_n, \mathcal{H}z_m \rangle, \quad m, n \in \{1, \ldots, M\}. \tag{24}$$

Furthermore, $E[\mathbf{v}\mathbf{v}^{\mathrm{H}}] = N_0\mathbf{A}$, where N_0 denotes the spectral power density of $v(t)$.

A baseband receiver may first compute the sufficient statistic $\mathbf{u}$ and pulse cross-correlation matrix $\mathbf{A}$, and second perform demodulation and decoding on the basis of (23). Figure 4 displays a generic inner receiver structure for producing estimates $\widehat{\mathbf{u}}$, $\widehat{\mathbf{A}}$ of $\mathbf{u}$, $\mathbf{A}$. Resorting to the TF domain, the coefficients (22) are computed as $\hat{u}_m = \langle \mathbf{Y} - \widehat{\mathbf{H}} \odot \mathbf{P}, \widehat{\mathbf{H}} \odot \mathbf{Z}^{(m)} \rangle$, and the cross-correlation terms (24) as $\hat{a}_{m,n} = \langle \widehat{\mathbf{H}} \odot \mathbf{Z}^{(n)}, \widehat{\mathbf{H}} \odot \mathbf{Z}^{(m)} \rangle$. The TF representation $\mathbf{Y}$ of the received signal $y(t)$ is obtained from a filter bank, while TF representations $\mathbf{Z}^{(1)}, \ldots, \mathbf{Z}^{(M)}$ of the elementary waveforms are provided by a local repository. These are mapped to TF representations $(\widehat{\mathbf{H}} \odot \mathbf{Z}^{(1)}), \ldots, (\widehat{\mathbf{H}} \odot \mathbf{Z}^{(M)})$ of $(\mathcal{H}z_1)(t), \ldots, (\mathcal{H}z_M)(t)$ by means of the channel model (10) discussed in Sect. 3. The aforementioned estimate $\widehat{\mathbf{H}}$ of the channel parameters needed for the mapping is provided by a channel estimator, which operates in the TF domain and takes as input the observation $\mathbf{Y}$ and a locally reproduced pilot signal representation $\mathbf{P}$ in a similar manner as channel estimators in OFDM receivers. Efficient channel parameter estimators operating on the basis of (21) are presented in [27].

Given $\mathbf{u}$, $\mathbf{A}$, and the codebook Ω, a number of standard decoding methods are available to the outer receiver on the basis of (23). Options for the estimation of the codeword $\mathbf{s} \in \Omega$ include

- the maximum-likelihood (ML) estimate given as $\hat{\mathbf{s}}_{\mathrm{ML}} = \arg\min_{\mathbf{s}\in\Omega} \mathbf{s}^{\mathrm{H}}\mathbf{A}\mathbf{s} - 2\Re(\mathbf{u}^{\mathrm{H}}\mathbf{s})$,
- the zero-forcing (ZF) based estimate given as $\hat{\mathbf{s}}_{\mathrm{ZF}} = \mathcal{D}(\mathbf{A}^{-1}\mathbf{u})$ with $\mathcal{D} : \mathbb{C}^M \to \Omega$ a certain detection rule,
- the linear minimum mean-squared error (MMSE) based estimate given as $\hat{\mathbf{s}}_{\mathrm{MMSE}} = \mathcal{D}((\mathbf{A} + \gamma^{-1}\mathbf{I}_M)^{-1}\mathbf{u})$,

with γ the ratio of the mean energy of the signals $s_1, \ldots, s_M$ over N_0.

Since the various inner receiver entities in Fig. 4 build on fixed algorithms they can be implemented in the form of reconfigurable hardware, being controlled through a limited number of parameters. One parameter may be appointed to select among a number of distinct analysis filter bank configurations, each relying on a Gabor system optimized for certain channel characteristics and signal formats. Further parameters may have the role of specifying the signal subsets to be provided by the two repositories, and the channel statistics needed by the channel estimator.

6. Receiver Configurations

The outlined receiver can principally be applied to all burst types featuring linear modulation and pilot/preamble signals. In the following, receiver configurations for DSSS and OFDM signals are discussed. Other forms of single-carrier and multi-carrier signals can be handled in similar ways. Through linearization even some nonlinear modulation schemes — such as Gaussian-filtered minimum shift keying adopted in the GSM (global system for mobile communications) standard — can be dealt with [28], but elaborating on this issue is out of the scope of this paper.

6.1 DSSS-Based Air Interfaces

Let us consider a DSSS signaling scenario where a burst comprises 2560 chips of duration $T_{\mathrm{chip}} = 260$ ns each, similar to a time slot in the *universal mobile telecommunications system terrestrial radio access* (UTRA) *frequency division duplex* (FDD) air interface. We further assume a spreading factor 16, resulting in $M = 160$ symbols per burst, randomly generated complex channelization/scrambling codes with elements from $\{\pm 1 \pm j\}$, and Q-ary quadrature amplitude modulation (QAM) with Gray encoding. Also randomly generated for every simulated burst reception is a realization of a doubly dispersive channel in line with the Gaussian WSSUS model with one/two-sided exponentially decaying delay/Doppler power spectra, with ν_{RMS} equal to 400 Hz and various τ_{RMS}. The flexible inner receiver proposed in Sect. 5

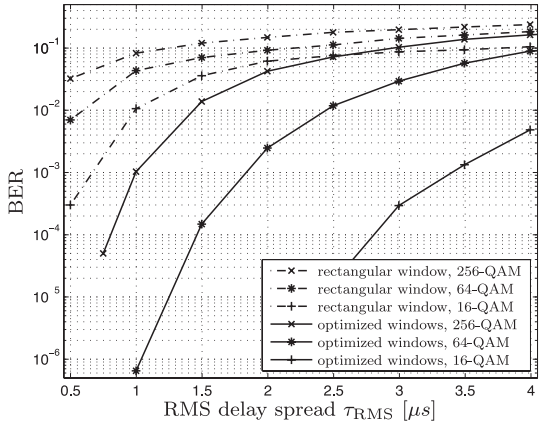

Fig. 5 BER performance of reconfigurable inner receiver in UTRA FDD compliant mode with perfect channel knowledge.

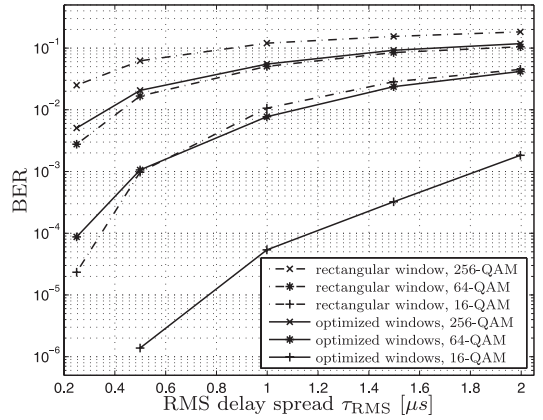

Fig. 6 BER performance of reconfigurable inner receiver in UTRA FDD compliant mode with pilot signal-based channel estimates.

is employed with the signal analysis operation configured as $T = 48 \cdot T_{\mathrm{chip}}$ and $TF = \frac{3}{4}$ along with optimized window functions. Since $F = 1/(64 \cdot T_{\mathrm{chip}})$ the signal analysis involves 128-point FFT computations at a double chip rate sampling. The outer receiver performs ZF and symbol detection. The observed bit error rates (BERs) in the absence of front end noise are shown in Fig. 5 for perfect channel estimation (i.e., $\widehat{\mathbf{H}} = \mathbf{H}$) and RMS delay spreads between $0.5\,\mu$s and $4\,\mu$s, and in Fig. 6 for computing $\widehat{\mathbf{H}}$ on the basis of an overlaid pilot signal with similar form and equal power as the information-bearing signal and τ_{RMS} between $0.25\,\mu$s and $2\,\mu$s. Choosing orthogonal channelization codes for the information and pilot signals, $\widehat{\mathbf{H}}$ is computed according to formula (15) in [27]. For comparison, the two figures also show the performance of a similar receiver based on block-wise DFT computations, that is, $T = 48 \cdot T_{\mathrm{chip}}$ and $TF = 1$ along with a rectangularly shaped window of length T.

The error rate performance can obviously be substantially improved through window optimization. Since no forward error correction is employed a BER of up to 10^{-3} may be acceptable. With optimized window functions and perfect channel knowledge this is achieved even with 256-QAM unless the RMS delay spread exceeds $1\,\mu$s, which is usually not the case in UTRA cells[†]. As in most receiver architectures deviations in the channel parameters resulting from pilot signal-based channel estimation have a dominant effect on the error rates, as seen in Fig. 6. Higher-order QAM may only be viable at smaller delay spreads, yet there is also a clear benefit from window optimization in scenarios with imperfect channel knowledge.

6.2 OFDM-Based Air Interfaces

Choosing T and F in line with the OFDM symbol length and subcarrier spacing, respectively, and further $g(t) \triangleq g_{\mathrm{rect}}^{(1/F)}(t)$ and $\mathbf{Z}_{(k,\ell)}^{(m)} \triangleq \delta_{k,k_m}\delta_{\ell,\ell_m}$ with $\delta_{m,n}$ the Kronecker delta and (k_m, ℓ_m) specifying the TF slot in which the mth information signal is conveyed, turns the structure in Fig. 4 into a conventional OFDM receiver. Here the discrete-time signal analysis corresponds to block-wise performed DFTs. Under the assumptions of proper TF synchronization, the delays of the essential signal parts not exceeding the guard period length $T_{\mathrm{g}} \triangleq T - 1/F$, and negligible Doppler dispersion, $\mathbf{H} \odot \mathbf{Z}^{(m)}$ perfectly represents $(\mathcal{H}z_m)(t)$ and the cross-correlation matrix $\mathbf{A}$ has the form of a diagonal matrix. The error rate performance of this receiver mode matches the performance of conventional OFDM receivers. Furthermore, the channel estimators presented in [27] reduce to OFDM channel estimators taking the second-order channel statistics into account, the performance of which is investigated in [30].

In this configuration, (1) does not represent a Gabor frame since $TF > 1$. This has to do with the fact that OFDM receivers disregard the signal parts in the guard periods. Alternative analysis filter bank configurations can evade the neglect of a fraction T_{g}/T of the signal power. However, the merit in terms of decoding performance does usually not outweigh the incurred cost in terms of complexity increase.

7. Conclusions

A generic baseband receiver architecture has been presented; it represents a generalization of the frequency domain signal processing concept known from OFDM receivers. By shifting from block-wise frequency domain processing to an appropriate TF processing the principal features of OFDM receivers, foremost the efficient handling of dispersive channels, are inherited and made applicable to arbitrary signals. The processing of signals without cyclic prefixes results in a certain error, the impact of which can be effectively limited by choosing optimized windows underlying the signal analysis operation. The case of DSSS signals in line with the UTRA FDD air interface specification has been studied as an example. We find that in typical urban and suburban environments the impact of the model error can be limited to acceptable levels through window

[†]In [29] RMS delay spreads of $0.17\,\mu$s for suburban and $0.65\,\mu$s for urban environments were found.

design, however, the performance degradation due to imperfect channel estimation may be considerable.

The possibility of employing efficient FFT algorithms for the filter bank implementation makes the generic receiver also competitive as far as complexity is concerned. The actual numbers of operations required for demodulating the signals associated with a particular air interface depend on the signal structure. However, in general the complexity can be assumed to be comparable to the complexity of corresponding single-mode receivers with frequency domain processing. Of course generality and reusability always come at a certain cost in error rate performance and/or complexity. Finally, it is worthwhile mentioning that the presented concepts for flexible *receiver* architectures carry over to corresponding flexible *transmitter* architectures to be used for instance for supporting heterogeneous air interfaces in a base station transceiver.

Acknowledgment

This work was supported by the European research project IST-27960 URANUS (Universal RAdio-link platform for efficieNt User-centric accesS).

References

[1] N. Lee, Linear Time-Frequency Representations for Transient Signal Detection, Ph.D. Thesis, Princeton University, 1995.
[2] H.G. Feichtinger and T. Strohmer, Gabor Analysis and Algorithms: Theory and Applications, Birkhäuser, Boston, MA, 1998.
[3] P.P. Vaidyanathan, Multirate Systems and Filter Banks, Prentice-Hall, Englewood Cliffs, NJ, 1993.
[4] T. Hunziker, Z. Ju, and D. Dahlhaus, "Efficient channel description in time-frequency domain with application to flexible radio," Proc. European Signal Processing Conf. (EUSIPCO'07), pp.866–870, Poznan, Poland, Sept. 2007.
[5] D. Falconer, S. Ariyavisitakul, A. Benyamin-Seeyar, and B. Eidson, "Frequency domain equalization for single-carrier broadband wireless systems," IEEE Commun. Mag., vol.40, pp.58–66, April 2002.
[6] H. Sari, G. Karam, and I. Jeanclaude, "Frequency-domain equalization of mobile radio and terrestrial broadcast channels," Proc. IEEE GLOBECOM'94, pp.1–5, San Francisco, CA, Nov. 1994.
[7] I. Martoyo, Frequency Domain Equalization in CDMA Detection, Ph.D. Thesis, Institut für Nachrichtentechnik, University of Karlsruhe, 1995.
[8] F. Adachi, A. Nakajima, K. Takeda, L. Liu, H. Tomeba, T. Yui, and K. Fukuda, "Frequency-domain equalisation for block CDMA transmission," European Transactions on Telecommunications, vol.19, pp.553–560, June 2008.
[9] W. Kozek and A.F. Molisch, "Nonorthogonal pulseshapes for multicarrier communications in doubly dispersive channels," IEEE J. Sel. Areas Commun., vol.16, no.8, pp.1579–1589, Oct. 1998.
[10] L. Vandendorpe, J. Louveaux, B. Maison, and A. Chevreuil, "About the asymptotic performance of MMSE MIMO DFE for filter-bank based multicarrier transmission," IEEE Trans. Commun., vol.47, no.10, pp.1472–1475, Oct. 1999.
[11] T. Hunziker and D. Dahlhaus, "Iterative detection for multicarrier transmission employing time-frequency concentrated pulses," IEEE Trans. Commun., vol.51, no.4, pp.641–651, April 2003.
[12] P. Jung and G. Wunder, "The WSSUS pulse design problem in multicarrier transmission," IEEE Trans. Commun., vol.55, no.10, pp.1918–1928, Oct. 2007.
[13] S.M. Phoong, Y. Chang, and C.Y. Chen, "DFT-modulated filterbank transceivers for multipath fading channels," IEEE Trans. Signal Process., vol.53, no.1, pp.182–192, Jan. 2005.
[14] P. Jung and G. Wunder, "On time-variant distortions in multicarrier transmission with application to frequency offsets and phase noise," IEEE Trans. Signal Process., vol.53, no.9, pp.1561–1570, Sept. 2005.
[15] P. Schniter, "A new approach to multicarrier pulse design for doubly-dispersive channels," Proc. Allerton Conf. Commun., Control, and Computing, Monticello, IL, Oct. 2003.
[16] W.K. Ma, P.C. Ching, and K.M. Wong, "Maximum likelihood detection for multicarrier systems employing non-orthogonal pulse shapes," Proc. IEEE Int. Conf. on Acoustics, Speech, and Signal Processing (ICASSP), pp.2489–2492, Istanbul, Turkey, June 2000.
[17] SDR Forum, SDRF Cognitive Radio Definitions, 2007. Working Document SDRF-06-R-0011-V1.0.0.
[18] M. Dillinger, K. Madani, and N. Alonistioti, Software Defined Radio: Architectures, Systems and Functions, John Wiley & Sons, West Sussex, England, 1993.
[19] H. Harada, Y. Kamio, and M. Fujise, "Multimode software radio system by parameter controlled and telecommunication component block embedded digital signal processing hardware," IEICE Trans. Commun., vol.E83-B, no.6, pp.1217–1228, June 2000.
[20] K. Gröchenig, Foundations of Time-Frequency Analysis, Birkhäuser, Boston, MA, 2001.
[21] P.A. Bello, "Characterization of randomly time-variant linear channels," IEEE Trans. Commun. Syst., vol.11, no.4, pp.360–393, Dec. 1963.
[22] H.G. Feichtinger, M. Hampejs, and G. Kracher, "Approximation of matrices by Gabor multipliers," IEEE Trans. Signal Process. Lett., vol.11, no.11, pp.883–886, Nov. 2004.
[23] A.W. Rihaczek, "Signal energy distribution in time and frequency," IEEE Trans. Inf. Theory, vol.14, no.3, pp.369–374, May 1968.
[24] H. Bölcskei and F. Hlawatsch, "Discrete Zak transforms, polyphase transforms, and applications," IEEE Trans. Signal Process., vol.45, no.4, pp.851–866, April 1997.
[25] Z. Ju, T. Hunziker, and D. Dahlhaus, "Time-frequency parameterization of doubly dispersive channels," Proc. European Signal Processing Conf. (EUSIPCO'09), Glasgow, Scotland, Aug. 2009.
[26] Z. Cvetkovic and M. Vetterli, "Tight Weyl-Heisenberg frames in $\ell^2(\mathbb{Z})$," IEEE Trans. Signal Process., vol.46, no.5, pp.1256–1259, May 1998.
[27] T. Hunziker and S. Stefanatos, "Efficient two-dimensional filters for doubly-dispersive channel estimation in time-frequency signal processing," Proc. Int. Symp. on Spread Spectrum Techn. and Appl. (ISSSTA'08), Bologna, Italy, Aug. 2008.
[28] J.W. Liang, B.C. Ng, J.T. Chen, and A. Paulraj, "GMSK linearization and structured channel estimate for GSM signals," Proc. IEEE Military Commun. Conf. (MILCOM'97), pp.817–821, Monterey, CA, Nov. 1997.
[29] G. Calcev, D. Chizhik, B. Göransson, S. Howard, H. Huang, A. Kogiantis, A.F. Molisch, A.L. Moustakas, D. Reed, and H. Xu, "A wideband spatial channel model for system-wide simulations," IEEE Trans. Veh. Technol., vol.56, no.2, pp.389–403, March 2007.
[30] P. Hoeher, S. Kaiser, and P. Robertson, "Two-dimensional pilot-symbol-aided channel estimation by Wiener filtering," Proc. IEEE Int. Conf. Acoustics, Speech, Signal Processing, pp.1845–1848, Munich, Germany, April 1997.

Appendix: Derivation of MSCE Formula

The MSCE can be written as

$$\varepsilon_{\mathrm{MSCE}}(g) = E\left[\left|\mathbf{H}_{(k,\ell)}\right|^2 \left|\langle x, g_{k,\ell}\rangle\right|^2\right] + E\left[\left|\langle \mathcal{H}x, g_{k,\ell}\rangle\right|^2\right] - 2\Re\left(E\left[\langle \mathcal{H}x, g_{k,\ell}\rangle \mathbf{H}^*_{(k,\ell)} \langle x, g_{k,\ell}\rangle^*\right]\right). \quad (\mathrm{A}\cdot 1)$$

The first two expectations from the left are equal to $\|g\|^2$ as follows from the unit channel gain and power spectral density of $x(t)$, and thus they are equal to TF. Using that $(\mathcal{H}x)(t) = \int_{-\infty}^{\infty}\int_{-\infty}^{\infty} C_{\mathcal{H}}(t,f)e^{j2\pi f(t-s)}x(s)dfds$ and (13), the third expectation can be rewritten as

$$
\begin{aligned}
&E\left[\langle \mathcal{H}x, g_{k,\ell}\rangle \mathbf{H}^*_{(k,\ell)} \langle x, g_{k,\ell}\rangle^*\right] \\
&= \int_{\mathbb{R}}\int_{\mathbb{R}} g^*_{k,\ell}(t) g_{k,\ell}(t') \int_{\mathbb{R}}\int_{\mathbb{R}} E\left[C_{\mathcal{H}}(t,f)\mathbf{H}^*_{(k,\ell)}\right] \\
&\quad E\left[x(s)x^*(t')\right] e^{j2\pi f(t-s)} dfdsdt'dt \qquad (\text{A}\cdot 2) \\
&= \int_{\mathbb{R}}\int_{\mathbb{R}} g^*_{k,\ell}(t) g_{k,\ell}(t') \int_{\mathbb{R}} R_{\mathcal{H}}(t-kT, f-\ell F) \\
&\quad e^{j2\pi f(t-t')} dfdt'dt \qquad (\text{A}\cdot 3) \\
&= \int_{\mathbb{R}}\int_{\mathbb{R}} g^*(t-kT) g(t'-kT) e^{j2\pi(t'-t)\ell F} \\
&\quad \int_{\mathbb{R}} R_{\mathcal{H}}(t-kT, f-\ell F) e^{j2\pi f(t-t')} dfdt'dt \qquad (\text{A}\cdot 4) \\
&= \int_{\mathbb{R}}\int_{\mathbb{R}} g^*(t-kT) g(t'-kT) \\
&\quad \int_{\mathbb{R}} R_{\mathcal{H}}(t-kT, f-\ell F) e^{j2\pi(f-\ell F)(t-t')} dfdt'dt \qquad (\text{A}\cdot 5) \\
&= \int_{\mathbb{R}}\int_{\mathbb{R}} g^*(t) g(t') \int_{\mathbb{R}} R_{\mathcal{H}}(t,f) e^{-j2\pi f(t'-t)} dfdt'dt \qquad (\text{A}\cdot 6) \\
&= \int_{\mathbb{R}}\int_{\mathbb{R}} g^*(t) \int_{\mathbb{R}} g(t-\tau) e^{j2\pi f\tau} d\tau R_{\mathcal{H}}(t,f) dtdf \qquad (\text{A}\cdot 7) \\
&= \int_{\mathbb{R}}\int_{\mathbb{R}} Z^*_g(t,f) R_{\mathcal{H}}(t,f) dtdf. \qquad (\text{A}\cdot 8)
\end{aligned}
$$

Inserting (A· 8) into (A· 1) leads to (12).

Thomas Hunziker received the Diploma and Ph.D. degrees in Electrical Engineering from the Swiss Federal Institute of Technology (ETH) Zurich in 1992 and 2002, respectively. From 2002 to 2006, he was a Visiting Researcher at the Advanced Telecommunications Research Institute International (ATR), Kyoto, Japan. He is now with the Communications Laboratory, University of Kassel, Germany. His research interests include OFDM and filter bank multicarrier systems, MIMO architectures, adaptive array signal processing, cross-layer design and medium access control in decentralized networks.

Ziyang Ju received the B.S. degree in Communications Engineering from Xidian University, China, in 2001, and the M.S. degree with distinction in communications technology from University of Ulm, Germany, in 2006. Since April 2006, she has been with the Communications Laboratory, University of Kassel, Germany, as a research assistant. Her research interests include time-frequency analysis and filter bank multicarrier systems.

Dirk Dahlhaus received the Diploma degree in Electrical Engineering from the University of Bochum, Germany, in 1992, and the Ph.D. from the Swiss Federal Institute of Technology (ETH) Zurich, Switzerland, in 1998. From 1999 until 2005 he was assistant professor for mobile radio at ETH Zurich. Since September 2005, he is full professor for communications at the University of Kassel, Germany. His reserach interests include different topics in the lower layers of mobile and wireless communication systems, e.g. statistical signal processing in multiuser and multiantenna systems.